Ge vacancies at Ge/Si interfaces: Stress-enhanced pairing distortion

Kentaro Takai,[1] Kenji Shiraishi,[1,3] and Atsushi Oshiyama[1,2,3]
[1]*Graduate School of Pure and Applied Sciences, University of Tsukuba, Tennodai, Tsukuba 305-8571, Japan*
[2]*Center for Computational Sciences, University of Tsukuba, Tennodai, Tsukuba 305-8577, Japan*
[3]*CREST, Japan Science and Technology Agency, 4-1-8 Honcho, Kawaguchi, Saitama 332-0012, Japan*
(Received 11 December 2006; revised manuscript received 30 August 2007; published 9 January 2008)

We have performed first-principles total-energy electronic-structure calculations based on the density-functional theory to clarify energetics and electron states of the Ge vacancies in strained Ge layers on the Si(001) surface. We find that pairing distortion is a principal relaxation pattern around the vacancies. The pairing of the two atoms located on either (110) or $(1\bar{1}0)$ plane is remarkably enhanced due to compressed strain in the lateral plane. It is found that the enhanced pairing causes reduction of formation energies, disappearance of deep levels in the monovacancy, deep-level crossing in the divacancy, and arrangement of the trivacancy on the (110) or the $(1\bar{1}0)$ plane. We have also found that the vacancy at the very interface layer facing the Si substrate is energetically unfavorable due to the larger energy cost to generate Si dangling bonds compared with Ge dangling bonds upon removal of atoms.

DOI: 10.1103/PhysRevB.77.045308 PACS number(s): 73.20.Hb, 68.47.Fg, 68.35.Dv, 68.55.Ln

I. INTRODUCTION

Heterostructures consisting of Si and Ge have been attracting great attention from both science and technology viewpoints. Two decades ago, two-dimensional hole gas and electron gas were observed in SiGe heterostructures,[1,2] leading to the first demonstration of bipolar and field-effect transistors made of the material in late 1980s.[3–5] Since then, a lot of research activities have been done regarding growth technique of lower-defect-density thin films and design of optimum structures for transistors.[6] Now, the observed enhanced mobility in strained Si, strained Ge, or strained Si_xGe_{1-x} is regarded as one of the promising boosters for postscaling Si technology.[6]

The strain that plays a key role in current technology comes from a 4% lattice mismatch between Si and Ge. The lattice mismatch itself is decisive in the growth mode of SiGe films. Ge growth on Si, for instance, exhibits a Stranski-Krastanov mode in which a few layers of Ge grow layer by layer (wetting), followed by three-dimensional islanding usually with stress releasing dislocations.[7] Yet, relations of thin-film morphology and growth conditions are less clarified for islanding processes. Several forms of strained pseudomorphic Ge thin films have been indeed observed at the early stage of island formation, depending on growth conditions.[8,9]

In spite of expanding knowledge of SiGe heterostructures, little is known, to our surprise, about atom-scale structures, particularly structures and energetics of point defects at the lattice mismatched strained interface. Point defects, though they belong to a minority, are generally known to play a decisive role in electronic properties of their mother materials and also nanoscale morphology of thin films. In a Ge film on Si, the most abundant and important point defect is expected to be Ge vacancy since Ge is larger than Si by 4% in lattice constant. Further, atomic structures and, therefore, electron states of vacancies should be sensitive to local strain. It is thus of fundamental importance to clarify behaviors of vacancies at SiGe stressed interfaces, which we discuss in this paper.

A monovacancy V_1 in covalent group IV semiconductors generally induces deep levels in the energy gap: In the ideal (i.e., unrelaxed) monovacancy with T_d symmetry, a triply degenerate t_2 level appears in the energy gap, whereas an a_1 state resonates near the valence-band top.[10–12] The t_2 level is partially occupied, depending on the charge state, i.e., $V_1^{2+}:a_1^2$, $V_1^{+}:a_1^2t_2^1$, $V_1^{0}:a_1^2t_2^2$, and $V_1^{-}:a_1^2t_2^3$, so that a symmetry-lowering lattice relaxation takes place (Jahn-Teller effect). Many of the experimental data on the Si monovacancy have been explained in terms of electron-state theory including Jahn-Teller pairing distortion.[13,14] As for Ge monovacancy, though less experimental data are available, similar pictures on deep levels seem to be valid, relying on the calculations.[12]

A divacancy V_2 in the bulk is also a usual point defect. The ideal divacancy has a D_{3d} symmetry and induces two doubly degenerate deep levels, e_u and e_g, in the energy gap, again being partially occupied depending on the charge state (i.e., $V_2^{+}:e_u^1$, $V_2^{0}:e_u^2$, and $V_2^{-}:e_u^3$). The symmetry-lowering lattice relaxation thus takes place. Actually, the pioneering electron spin resonance (EPR) experiments[15] performed for Si have revealed that V_2 with either positive or negative charge has the lower symmetry of C_{2h}. As for the actual relaxation pattern of surrounding atoms, two possibilities have been proposed: The pairing distortion proposed on the basis of the EPR data[15] and the resonant bond distortion proposed from the density-functional theory.[16] A lot of efforts, mainly from the theoretical side, to clarify the relaxation pattern have been done.[17–24] Yet, it is still controversial.

The SiGe interface offers a new stage for lattice relaxation around the vacancy. Stress inherent in the interface, as well as difference in chemical elements, is likely to affect atom-scale relaxation patterns and, therefore, electron states near the energy gap. It is thus of importance to clarify salient features of vacancies near the SiGe interface.

In the present paper, we have performed total-energy electronic-structure calculations based on the density-functional theory for neutral as well as charged vacancies in Ge pseudomorphic thin films on Si(001) substrates. We focus on Ge monovacancy, divacancy, and trivacancy in laterally

compressed Ge thin films. We have found that the particular pairing distortion, where two neighboring atoms located on either (110) or $(1\bar{1}0)$ plane are rebonded, plays principal roles in atom-scale relaxation patterns in the vacancies. This is due to the compressive lateral strain inherent in the Ge film on Si. In the case of Ge monovacancy, the lengths of the rebonds are longer than the ideal bond length in the Ge crystal only by 12–14%, implying that no deep level is induced by the monovacancy. For the Ge divacancy, the large pairing distortion where deep levels cross due to the pairing is found to be realized, shedding light on the controversy about the structure of V_2 in the bulk Si and Ge. The most stable trivacancy is found to be arranged on the (110) or the $(1\bar{1}0)$ plane, which is again due to the lateral strain in the Ge film. Effects of chemical difference between Si and Ge are also clarified.

The organization of the paper is as follows. In Sec. II, our calculational method is briefly described. In Sec. III, calculated results for the Ge monovacancy, divacancy, and trivacancy are presented. Section IV concludes the paper.

II. CALCULATIONS

Total-energy electronic-structure calculations have been performed based on the density-functional theory.[25,26] The local density approximation (LDA) based on the diffusion Monte Carlo calculations for the electron gas[27] is used, as is parametrized by Perdew and Zunger,[28] for exchange-correlation energy. To examine the validity of LDA, we have also performed the calculations using generalized gradient approximation (GGA)[29] for the monovacancy.

Nuclei and core electrons are simulated by norm-conserving pseudopotentials generated by the Troullier-Martins scheme.[30] We regard $3s$ and $3p$ orbitals of Si and $4s$ and $4p$ orbitals of Ge as valence states. Nonlocality for both s and p potentials is considered. We have examined transferability of the pseudopotentials by changing core radii r_c, and compare structural and vibrational properties of SiH_4 and GeH_4 molecules as well as Si and Ge crystals, as described below. We use $r_c=1.8a_0$ for s and p orbitals of Si, $r_c=1.9a_0$ for s and p of Ge, where a_0 is a Bohr radius. We have also prepared the pseudopotential for hydrogen for our slab model, where we take $r_c=1.5a_0$ for $1s$ orbital of H.

Kohn-Sham states and, therefore, electron densities are expanded in terms of a plane-wave basis set. Kohn-Sham states are obtained by minimization of the Kohn-Sham orbital energies with a conjugate-gradient technique.[14] The cutoff energy E_c of the plane-wave basis set is determined by calculating total energies of several prototype materials with changing E_c from 7 to 30 Ry. We have found that $E_c=9$ Ry is enough to assure the convergence within 1% in the relative total energies. Calculated bond lengths of SiH_4, GeH_4, Si crystal, and Ge crystal using the calculational parameters r_c and E_c agree with the experimental values within 1.0%, 2.0%, 0.1%, and 0.2%, respectively. Calculated vibrational frequencies and bulk modulus of these materials are also in agreement with the experimental values within several percent.

We use a repeating slab model that contains five Si and nine Ge atomic layers plus a vacuum region of 8.1 Å thickness in a unit cell. Convergence with respect to the slab thickness has been examined by using thicker slabs containing up to six Si layers and ten Ge layers. It is found that calculated defect formation energies converge within less than 0.1 eV. The outermost atomic layers are terminated by hydrogen atoms. The unit cell size in the lateral plane is taken as $c(6\times6)$. The lateral cell size has been also examined by changing the size from $c(4\times4)$ to $c(8\times8)$. It is found that the formation energies of monovacancy, divacancy, and trivacancy converge within less than 0.1, 0.2, and 0.2 eV with $c(6\times6)$, respectively. The lattice constants in lateral directions are fixed to the theoretical lattice constants of Si, which mimics the Ge thin film on the Si substrate. The Γ-point sampling for the two-dimensional Brillouin-zone summation is found to be enough after examination of convergence in total-energy differences.

The atomic positions of the bottom-most Si atoms as well as the H atoms attached are fixed to their ideal positions. The atomic positions of the uppermost Ge atoms and the H atoms attached are allowed to relax only in [001] directions. Positions of other atoms are fully relaxed by the conjugate-gradient minimization technique using calculated Helmann-Feynman forces. Forces acting on atoms in optimized geometries are less than 5.1×10^{-2} eV/Å.

In our slab model, the calculated lattice mismatch between Si and Ge is 4.1%, which nicely reproduces the experimental value of 4.2%. Further, the calculated valence-band offset is 0.7 eV, which quantitatively agrees with the experimental and theoretical values.[31–33]

III. RESULTS AND DISCUSSION

In this section, we present atomic structures and energetics for Ge monovacancies, divacancies, and trivacancies at the Ge/Si interface obtained by our LDA calculations. In addition, we discuss electron states for monovacancies and divacancies. Strained pseudomorphic Ge thin films on Si(001) are simulated by Ge/Si slabs, with the lateral lattice constant being fixed to the theoretical value for bulk Si, 5.43 Å. Geometry optimization for the slab without the vacancy leads to atomic relaxation along the [001] direction in Ge regions. As a result, the Ge atomic-layer distance along [001] becomes 1.45 Å, which is larger than the corresponding value of 1.41 Å in bulk strain-free Ge. This is obviously due to compressive strain in the lateral plane.

We consider how the formation energy of the vacancy depends on the atomic layers where the vacant sites are generated. We thus examine the four monovacancies, i.e., the monovacancy at the first Ge interface layer $V_1^{(1)}$, at the second Ge interface layer $V_1^{(2)}$, at the third Ge interface layer $V_1^{(3)}$, and at the fourth Ge interface layer $V_1^{(4)}$, as is illustrated in Fig. 1(a). Similar for the divacancy, we examine three possibilities: The divacancy at the first and second layers $V_2^{(12)}$, at the second and third layers $V_2^{(23)}$, and at the third and fourth layers $V_2^{(34)}$ [Fig. 1(b)]. As for the trivacancy, we examine seven possibilities. When we use the symbol $V_3^{(ijk)}$ to

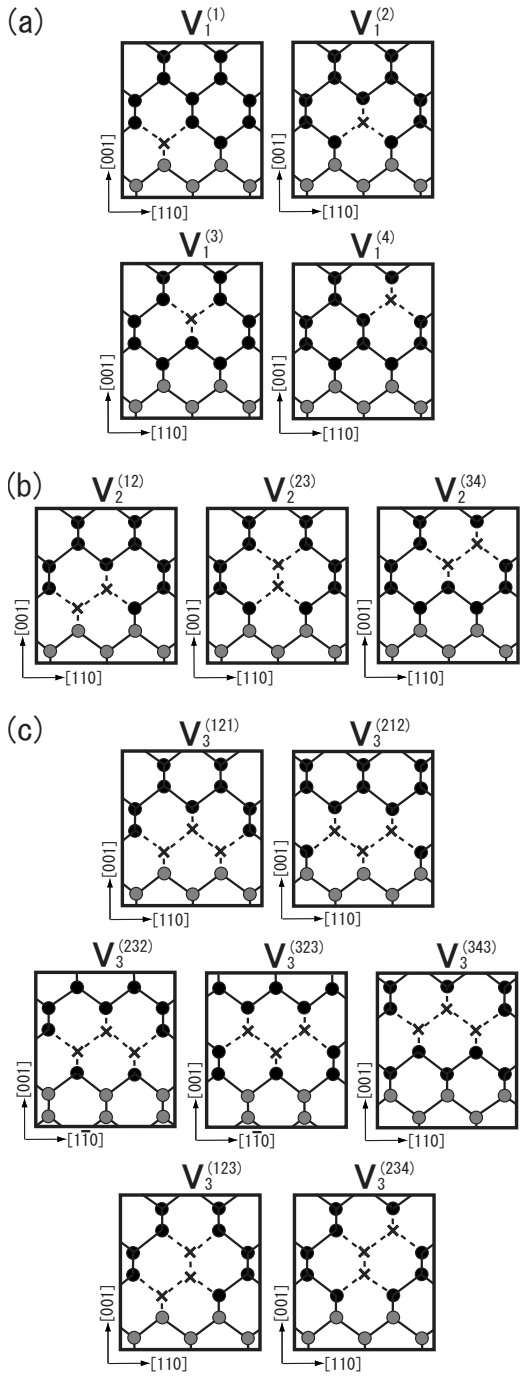

FIG. 1. Schematic view of several (a) monovacancies V_1, (b) divacancies V_2, and (c) trivacancies V_3, in the slab model. Gray and black balls represent Si and Ge atoms, respectively. Vacant sites are depicted by crosses.

denote the trivacancy in which the first atomic site at the ith Ge layer, the second atomic site at the jth layer, and the third atomic site at the kth layer are removed, we have $V_3^{(121)}$, $V_3^{(212)}$, $V_3^{(232)}$, $V_3^{(323)}$, $V_3^{(343)}$, $V_3^{(123)}$, and $V_3^{(234)}$ [Fig. 1(c)]. These seven configurations cover all the possibilities of arrangements of adjacent three vacant sites. When the number of vacant sites increases, the degree of freedom increases so that some peculiar configurations, such as fourfold coordinated geometries around the vacant sites,[34] may be possible.

TABLE I. Calculated interatomic distances among four nearest neighbor atoms around V_1 at each atomic layer. The distances around V_1 in strain-free Ge (sf Ge) and biaxially compressed Ge (bc Ge) calculated using the 216-site supercell ($V_1^{(216\ \text{sites})}$) in both LDA and GGA are also shown. d_{ij} indicates the distance in Å between ith and jth atoms labeled in Fig. 2(a). In the unrelaxed geometries, $d_{12}=d_{34}=3.84$ Å and $d_{13}=d_{14}=d_{23}=d_{24}=3.95$ Å for $V_1^{(1)}$. For unrelaxed $V_1^{(2)}$, $V_1^{(3)}$, and $V_1^{(4)}$, $d_{13}=d_{14}=d_{23}=d_{24}=3.97$ Å, whereas $d_{12}=d_{34}=3.84$ Å.

	d_{12}	d_{34}	d_{13}	d_{14}	d_{23}	d_{24}
$V_1^{(1)}$	2.80	2.81	3.42	3.42	3.42	3.42
$V_1^{(2)}$	2.85	2.81	3.48	3.48	3.48	3.48
$V_1^{(3)}$	2.82	2.83	3.45	3.45	3.47	3.47
$V_1^{(4)}$	2.81	2.83	3.48	3.49	3.48	3.48
In bc Ge						
$V_1^{(216\ \text{sites})}$ LDA	2.81	2.80	3.44	3.44	3.45	3.45
$V_1^{(216\ \text{sites})}$ GGA	2.97	2.97	3.72	3.72	3.72	3.71
In sf Ge						
$V_1^{(216\ \text{sites})}$ LDA	3.15	3.15	3.45	3.45	3.45	3.45
	3.40[a]	3.40[a]	3.55[a]	3.54[a]	3.55[a]	3.54[a]
	3.53[b]	3.53[b]	3.89[b]	3.89[b]	3.89[b]	3.89[b]
$V_1^{(216\ \text{sites})}$ GGA	3.29	3.29	3.59	3.60	3.60	3.60

[a]Reference 12.
[b]Reference 21.

Yet, we restrict ourselves to the usual trivacancy and examine the relaxation pattern and energetics in this paper.

To discuss the stable forms of these vacancies, we calculate the formation energy $E_f(n)$. Here, $E_f(n)$ for the vacancy, which contains n-vacant sites, is expressed as

$$E_f(n) = E(n) - E_0 + n\mu_{\text{Ge}},$$

where $E(n)$ and E_0 are the total energies of the corresponding slabs with and without vacant sites, respectively, and μ_{Ge} is the chemical potential of Ge for which we take the value in the Ge bulk crystal.

A. Monovacancy

We first discuss structural characteristics of Ge monovacancies at each atomic layer. Table I shows calculated interatomic distances among four nearest neighbors of V_1 in the total-energy minimized configurations along with corresponding distances for V_1 in bulk strain-free Ge. We have found that pairing distortion is a principal relaxation pattern around the monovacancy. In particular, pairing of the two atoms located on either the (110) or the (1$\bar{1}$0) plane is remarkably enhanced: As shown in Table I and Fig. 2(a), the pairing between the two atoms 1 and 2, or 3 and 4, which are located on the same Ge layer perpendicular to the [001] direction, is enhanced so that the distances of the two atoms are shorter than the pairing distance of V_1 in bulk strain-free Ge by 10–13% (Table I). The lengths of these rebonds are longer than the ideal Ge–Ge bond length in the Ge crystal

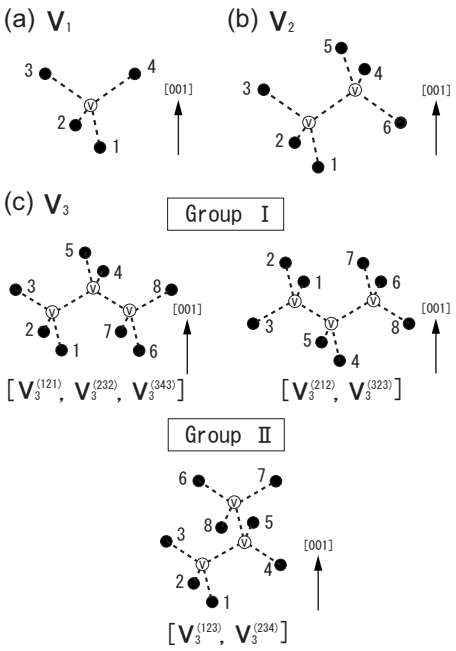

FIG. 2. The atomic configurations of the ideal vacancies: (a) monovacancy (V_1) with the four nearest neighbor atoms, (b) divacancy (V_2) with the six nearest neighbor atoms, and (c) trivacancies with the eight nearest neighbor atoms. Black and white balls represent the nearest neighbor atoms and vacant sites, respectively.

only by 12–14%. This remarkable enhancement of the pairing is due to the compressed strain in the lateral plane that is inherent in the strained Ge thin film on the Si(001) substrate.

Calculated formation energies of monovacancies are shown in Table II along with the formation energy of the monovacancy in bulk strain-free Ge. We have found that the formation energies in the present strained Ge, which range from 1.4 to 2.2 eV, are substantially smaller than the corresponding value (2.7 eV) in bulk Ge. The calculated formation energy for an ideal (unrelaxed) $V_1^{(4)}$ is 3.4 eV, which is comparable with the formation energy of 3.5 eV for an ideal V_1 in bulk strain-free Ge. This indicates that energy gain due to pairing relaxation is surprisingly larger in strained Ge than in bulk Ge: 2.0 eV for $V_1^{(4)}$, for instance. Lateral strain causes this enhancement of the pairing and, thus, reduction of formation energies.

For the monovacancies at several Ge interface layers, we have found that the monovacancy, which has the two nearest neighbor Si atoms around the vacant site, has the maximum formation energy of 2.2 eV (Table II). This is a consequence of larger energy cost to generate Si dangling bonds compared with Ge dangling bonds: Even though dangling bonds are partly connected after the pairing relaxation, their original orbital energies affect the formation energies of the vacancies. The dangling bond energy $\varepsilon_{\mathrm{db}}$ defined as $\varepsilon_{\mathrm{db}}=(\varepsilon_s+3\varepsilon_p)/4$, where ε_s and ε_p are s and p, respectively, orbital energies, is −5.84 eV for Si and −5.96 eV for Ge.

It is occasionally found that LDA overestimates the binding energy compared with GGA. In order to examine the validity of LDA, we have also performed the GGA calculations for V_1 in bulk strain-free Ge and in biaxially compressed Ge by 4.1%. The calculated results are tabulated in Tables I and II. We have found that the pairing distances in biaxially compressed Ge and in strain-free Ge are 2.97 and 3.29 Å, respectively in GGA. The corresponding LDA values are 2.81 and 3.15 Å, respectively. Hence, we can conclude that the enhanced pairing obtained by LDA is valid even if we use GGA, although the rebond length has an ambiguity of 0.1 Å. As for the formation energies, the calculated values for the monovacancy in the compressed Ge are 1.6 eV in both LDA and in GGA, whereas the corresponding values in strain-free Ge are 2.7 eV in LDA and 2.9 eV in GGA. Again, it is found that GGA gives essentially the same results as LDA does.

TABLE II. Calculated formation energies $E_f(1)$ of monovacancies, $E_f(2)$ of divacancies, and $E_f(3)$ of trivacancies in units of eV with the number of the nearest neighbor Si atoms N_{Si}. Formation energies of monovacancies in both biaxially compressed Ge (bc Ge) and in strain-free Ge (sf Ge) obtained by 216-site supercell calculations ($V_1^{(216\ \mathrm{sites})}$) are also shown (Ref. 35).

V_1	$V_1^{(1)}$	$V_1^{(2)}$	$V_1^{(3)}$	$V_1^{(4)}$	
$E_f(1)$	2.2	1.6	1.5	1.4	
N_{Si}	2	0	0	0	
V_2	$V_2^{(12)}$	$V_2^{(23)}$	$V_2^{(34)}$		
$E_f(2)$	3.5	3.0	2.8		
N_{Si}	2	0	0		
V_3 Group I	$V_3^{(121)}$	$V_3^{(212)}$	$V_3^{(232)}$	$V_3^{(323)}$	$V_3^{(343)}$
$E_f(3)$	4.8	4.4	3.9	3.9	3.6
V_3 Group II		$V_3^{(123)}$	$V_3^{(234)}$		
$E_f(3)$		4.9	4.3		
N_{Si}	4	2	0	0	0

$V_1^{(216\ \mathrm{sites})}$	In bc Ge		In sf Ge	
	LDA	GGA	LDA	GGA
$E_f(1)$	1.6	1.6	2.7	2.9

The large pairing distortion that we have found causes unusual electron states. In the neutral monovacancy in bulk Ge, the pairing distortion takes place so that the T_d symmetry is lowered to the D_{2d} symmetry, and the deep-level t_2 splits into b_2 and doubly degenerate e states. The amount of the splitting is a few tenths of eV.[12] In the neutral state, two electrons are accommodated in the b_2 state, whereas the e state is empty. In the Ge/Si(001) system, a chemical difference between Ge and Si, as well as a lateral strain, lowers the symmetry to C_{2v} even in the unrelaxed monovacancy, where b_1 and b_2 states corresponding to e in the D_{2d} symmetry are almost degenerate and the a_1' state corresponding to b_2 in the D_{2d} symmetry appears at about 0.3 eV below the b_1 and b_2 states; the three levels are located in the energy gap. The large pairing distortion enhanced by the compressive lateral strain makes the three levels split significantly so that the a_1'

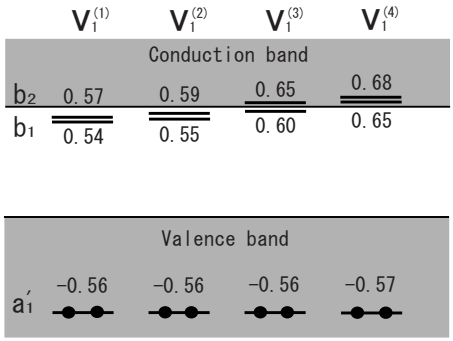

FIG. 3. Calculated energy levels induced by the monovacancy at each atomic layer with respect to the valence band edges in units of eV. The level occupation is given by the number of filled circles. The a_1' states are resonant in the valence bands, showing less localized characters compared with b_1 and b_2 states.

state, which has a bonding character of paired atoms, is located in valence bands. The states b_1 and b_2, which have antibonding characters, on the other hand, shift upward substantially. We have analyzed Kohn-Sham orbitals carefully to identify characters of obtained electron states. Figure 3 shows the calculated energy levels a_1', b_1, and b_2. It is surprising that the splitting due to the pairing is about 1 eV. This large splitting gives the b_1 and b_2 states located near the conduction band bottom,[36] leading to a possibility that deep levels can be erased in strained thin films. Yet, more elaborate calculations beyond LDA are necessary to obtain a definite conclusion as to the level positions of the two states.

The large splitting due to the enhanced pairing substantially affects the energetics among different charge states. Figure 4 shows calculated formation energies as a function of the Fermi-level position for various charge states of the monovacancy placed at the fourth Ge layer $V_1^{(4)}$. It is found that the neutral charge state (0) is most stable for a wide range of the Fermi-level position in the band gap. The occupancy level between the neutral (0) and negatively charged (−) states is located near the conduction-band bottom: i.e., (0/−)=0.63 eV. The doubly negatively charged state (2−) is found to be metastable for any position of the Fermi level. These energetics in strained Ge are in sharp contrast with the

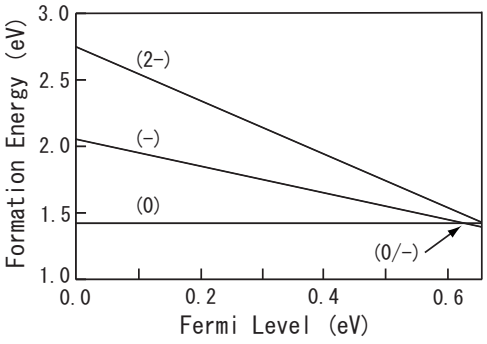

FIG. 4. Formation energies of monovacancy at the fourth Ge layer $V_1^{(4)}$ for the different charge states as a function of the Fermi-level position in the energy gap. The Fermi level is measured from the top of the valence bands. The arrow indicates the (0/−) ionization energy.

TABLE III. Calculated interatomic distances among six nearest neighbor atoms around V_2 at each atomic layer. d_{ij} indicates the distance in Å between ith and jth atoms labeled in Fig. 2(b). In the ideal geometries, $d_{12}=d_{45}=3.84$ Å and $d_{13}=d_{23}=d_{46}=d_{56}=3.98$ Å in $V_2^{(23)}$ and $V_2^{(34)}$, whereas $d_{13}=d_{23}=3.95$ Å and $d_{46}=d_{56}=3.98$ Å in $V_2^{(12)}$, with other distances being the same.

	d_{12}	d_{13}	d_{23}	d_{45}	d_{46}	d_{56}
$V_2^{(12)}$	2.70	3.31	3.31	2.75	3.42	3.42
$V_2^{(23)}$	2.79	3.42	3.42	2.78	3.40	3.40
$V_2^{(34)}$	2.74	3.37	3.40	2.76	3.39	3.40

corresponding energetics in bulk strain-free Ge where a variety of charge states from (2+) to (2−) are most stable depending on the Fermi-level position.[12] This significant modification in strained Ge is due to the large splitting between the a_1' state and the b_1 and b_2 states owing to the enhanced pairing, as discussed above.

There are no experimental data available that directly support the enhanced pairing and the reduced formation energy of the vacancy. However, Rutherford backscattering experiments performed for strained Si on $Si_{0.8}Ge_{0.2}$ (Ref. 37) imply the decrease of the vacancy formation energy. In this experimental situation, strained Si is contracted along the direction perpendicular to the interface, and pairing enhancement may be possible in the direction. Strain-induced enhancement of the pairing relaxation that we have found may be consistent with this experiment, although detailed analysis is required.

B. Divacancy

Table III shows calculated interatomic distances among six nearest neighbors of V_2 in the total-energy minimized configurations. We have found that pairing distortion is a principal relaxation pattern around the divacancy, similar to the monovacancy case. The pairing of the two atoms located on either the (110) or the $(1\bar{1}0)$ plane is remarkably enhanced: As shown in Table III and Fig. 2(b), the pairing between the two atoms 1 and 2, or 4 and 5, which are located on the same Ge layer perpendicular to the [001] direction, is enhanced. The lengths of such enhanced rebonds are 2.70–2.79 Å, which are shorter than the corresponding value in Ge bulk, 3.60 Å,[21] by almost 30%. We have also examined the possibility of the resonant bond configuration: We start with the resonant bond geometry and fully relaxed it; the final geometry we have obtained is the pairing geometry. Hence, it is concluded that the resonant bond configuration is highly unlikely in the strained Ge films due to lateral strain.

Table II shows calculated formation energies of $V_2^{(12)}$, $V_2^{(23)}$, and $V_2^{(34)}$ in Ge strained layers. We have found that the formation energy is the highest when the divacancy has the two nearest neighbor Si atoms around the vacant sites. This is due to larger energy cost to generate Si dangling bonds compared with Ge dangling bonds in the unrelaxed divacancies. A comparison of the formation energies of mono- and divacancies leads to a conclusion that the binding energies of the two monovacancies are 0.1–0.3 eV in the laterally

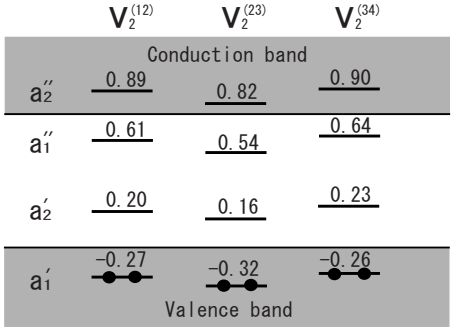

FIG. 5. Calculated energy levels of the divacancies at each atomic layer with respect to the valence-band top in units of eV. The level occupation is given by the number of filled circles.

strained Ge film. This binding energies are substantially smaller than the corresponding value (almost 2 eV) in bulk Si.[18,38,39]

The enhanced pairing distortion causes deep-level structures different from those in bulk strain-free Ge. Figure 5 shows an obtained electronic structure near the energy gap. In the neutral divacancy in bulk Ge, the symmetry-lowering lattice relaxation in which the D_{3d} symmetry is lowered to the C_{2h} symmetry takes place so that the deep-level e_u splits into b_u and a_u states and another deep-level e_g splits into a_g and b_g states. It has been proposed that the possible relaxation patterns are the pairing distortion and the resonant bond distortion. In the neutral state, two electrons are accommodated in the b_u state in the pairing configuration, whereas two electrons are accommodated in the a_u state in the resonant bond configuration.[16,18,21] In the Ge/Si(001) system, the chemical difference between Ge and Si, as well as lateral strain, lowers the symmetry to C_s even in the ideal divacancy, where a_1' (a_2') and a_1'' (a_2'') states located in the energy gap correspond to e_u (e_g) in the D_{3d} symmetry. The a_2' and a_2'' states are almost degenerate, and the a_1' and a_1'' states split by 0.1–0.2 eV in the ideal divacancy. We have found that the pairing distortion makes a_1' and a_1'' or a_2' and a_2'' states split substantially. The splitting is so large that the upper state (a_1'') from the lower pair (a_1' and a_1'') is located above the lower state (a_2') from the upper pair (a_2' and a_2''), and the a_1'' and a_2'' states, which have antibonding characters of paired atoms, shift upward substantially. This deep-level crossing is not realized in bulk strain-free Ge.[21]

C. Trivacancy

For the trivacancy, we investigate seven possible configurations of vacant sites [Fig. 1(c)]. The seven configurations are classified into two groups. One group consists of $V_3^{(121)}$, $V_3^{(212)}$, $V_3^{(232)}$, $V_3^{(323)}$, and $V_3^{(343)}$, which are arranged on the (110) or the $(1\bar{1}0)$ plane (group I). The other group is $V_3^{(123)}$ and $V_3^{(234)}$, where vacant sites are arranged on the (101), $(10\bar{1})$, (011), or $(01\bar{1})$ plane (group II) [Fig. 2(c)].

Table IV shows calculated interatomic distances among eight nearest neighbors of V_3 in the total-energy minimized configurations. Again, we have found that pairing distortion is a principal relaxation pattern around the trivacancy, similar to the monovacancy and divacancy cases. The pairing of the two atoms located on either the (110) or the $(1\bar{1}0)$ plane is remarkably enhanced: As shown in Table IV and Fig. 2(c), the three pairings between the two atoms 1 and 2, 4 and 5, and 6 and 7 in the trivacancies in group I are enhanced, whereas the two pairings between 1 and 2, and 6 and 7 are enhanced in group II. The lengths of such enhanced rebonds are 2.66–2.80 Å. As in the mono- and divacancies, the compressed strain in the lateral plane inherent in the Ge thin films causes the enhanced pairing distortion.

TABLE IV. Calculated interatomic distances among eight nearest neighbor atoms around V_3. d_{ij} indicates the distance in Å between ith and jth atoms labeled in Fig. 2(c). In the ideal geometries, d_{12} and d_{67} are 3.84 Å, d_{45} is 3.84 or 3.98 Å, and d_{13}, d_{23}, d_{68}, and d_{78} are 3.95 or 3.98 Å.

	d_{12}	d_{13}	d_{23}	d_{45}	d_{67}	d_{68}	d_{78}
				Group I			
$V_3^{(121)}$	2.66	3.32	3.32	2.72	2.67	3.32	3.32
$V_3^{(212)}$	2.73	3.42	3.42	2.68	2.73	3.42	3.42
$V_3^{(232)}$	2.75	3.42	3.43	2.73	2.74	3.42	3.42
$V_3^{(323)}$	2.74	3.39	3.39	2.74	2.74	3.39	3.40
$V_3^{(343)}$	2.70	3.39	3.40	2.70	2.70	3.39	3.40
				Group II			
$V_3^{(123)}$	2.73	3.29	3.14	3.12	2.76	3.33	3.32
$V_3^{(234)}$	2.80	3.32	3.36	3.10	2.78	3.38	3.24

Table II shows calculated formation energies of trivacancies in Ge strained layers. We have found that the formation energies are larger when the vacancies have more nearest neighbor Si atoms around the vacant sites: The formation energy of $V_3^{(121)}$, which has the four nearest neighbor Si atoms around vacant sites, is the largest and that of $V_3^{(212)}$, which has the two nearest neighbor Si atoms, is the second largest in group I, whereas that of $V_3^{(123)}$, which has the two nearest neighbor Si atoms, is the largest in group II. This is due to larger energy cost to generate Si dangling bonds compared with Ge dangling bonds in the unrelaxed vacancies.

Comparing the formation energies of trivacancies, which have the same number of the nearest neighbor Si atoms around vacant sites in groups I and II, we have found that the formation energies for the former group are lower than those for the latter group by 0.4–0.7 eV. This is due to the enhanced pairing of the neighboring atoms located on either the (110) or the $(1\bar{1}0)$ plane: In group I, there are three enhanced pairings, whereas there are two in group II.

Table V shows the energy gains ΔE associated with the trivacancy formation processes, $V_1+V_2 \rightarrow V_3$. It is found that the energy gains are 0.6–0.9 eV for group I and that they are less than 0.3 eV for group II. The result shows that trivacancy, which is arranged on the (110) or the $(1\bar{1}0)$ plane, is energetically favorable. It is again due to the lateral strain in the Ge film.

IV. CONCLUSION

We have performed the total-energy electronic-structure calculations based on the density-functional theory that pro-

TABLE V. Calculated energy gains ΔE of several trivacancy formation processes, $V_1+V_2\rightarrow V_3$, in units of eV. For the group II case, there are two possible processes: (a) $V_1^{(i)}+V_2^{(jk)}\rightarrow V_3^{(ijk)}$ and (b) $V_1^{(k)}+V_2^{(ij)}\rightarrow V_3^{(ijk)}$.

Group I	$V_3^{(121)}$	$V_3^{(212)}$	$V_3^{(232)}$	$V_3^{(323)}$	$V_3^{(343)}$
ΔE	0.9	0.7	0.7	0.6	0.6
Group II	$V_3^{(123)}$	$V_3^{(234)}$			
ΔE (a)	0.3	0.1			
ΔE (b)	0.1	0.1			

vides a firm theoretical framework to discuss energetics and electron states of the intrinsic defects in strained Ge layers at the Ge/Si(001) interface.

For each Ge vacancy (monovacancy, divacancy, and trivacancy), we have found that pairing distortion is a principal relaxation pattern around the vacancies. The pairing of the two atoms located on either the (110) or the $(1\bar{1}0)$ plane is remarkably enhanced. This is a consequence of the compressed strain in the lateral plane that is inherent in the strained Ge thin film on the Si(001) substrate. The enhanced pairing causes a substantial reduction of the formation energies of the monovacancies in the strained Ge layer compared with the corresponding value in bulk strain-free Ge. Furthermore, this enhancement of the pairing also renders a particular type of trivacancies energetically favorable. The calculated formation energies for trivacancies arranged on the (110) or the $(1\bar{1}0)$ plane are substantially smaller than those of other trivacancies.

A detailed comparison of formation energies for vacancies leads to a conclusion that the vacancy at the very interface layer facing the Si substrate is energetically unfavorable due to the larger energy cost to generate Si dangling bonds compared with Ge dangling bonds upon removal of atoms.

We have also investigated the electronic structure for the monovacancies and divacancies. It is found that the enhanced pairing substantially affects the electronic structure. In the monovacancies, deep levels induced in unrelaxed geometry split by about 1 eV upon pairing, leading to disappearance of the deep levels. As a consequence, the charged monovacancy is found to be energetically unfavorable for most values of the Fermi energy in the band gap. In the divacancies, the enhanced pairing distortion causes the deep-level crossing, which is not realized in bulk strain-free Ge.

ACKNOWLEDGMENTS

The present work was partly supported by Grants-in-Aid for Scientific Research from the Ministry of Education, Culture, Sports, Science and Technology, Japan under Contract Nos. 17064002, 16310083, 18360017, and 18063003. Computations were done at the Academic Computing and Communications Center, University of Tsukuba, at the Research Center for Computational Science, National Institutes of Natural Sciences, and at the Institute for Solid State Physics, University of Tokyo.

[1] R. People, J. C. Bean, D. V. Lang, A. M. Sergent, H. L. Störmer, K. W. Wecht, R. T. Lynch, and K. Baldwin, Appl. Phys. Lett. **45**, 1231 (1984).
[2] G. Abstreiter, H. Brugger, T. Wolf, H. Jorke, and H. J. Herzog, Phys. Rev. Lett. **54**, 2441 (1985).
[3] G. L. Patton, S. S. Iyer, S. L. Delage, S. Tiwari, and J. M. C. Stork, IEEE Electron Device Lett. **9**, 165 (1988).
[4] D. K. Nayak, J. C. S. Woo, J. S. Park, K.-L. Wang, and K. P. MacWilliams, IEEE Electron Device Lett. **12**, 154 (1991); S. Verdonckt-Vandebroek, E. F. Crabbé, B. S. Meyerson, D. L. Harame, P. J. Restle, J. M. C. Stork, A. C. Megdanis, C. L. Stanis, A. A. Bright, G. M. W. Kroesen, and A. C. Warren, *ibid.* **12**, 447 (1991).
[5] S. Subbanna, V. P. Kesan, M. J. Tejwani, P. J. Restle, D. J. Mis, and S. S. Iyer, Symposium on VLSI Technology Digests of Technical Papers, Kyoto, Japan, 1991, pp. 103–104; V. P. Kesan, S. Subbanna, P. J. Restle, M. J. Tejwani, J. M. Aitken, S. S. Iyer, and J. A. Ott, Tech. Dig. - Int. Electron Devices Meeting, 25 (1991); P. M. Garone, V. Venkataraman, and J. C. Sturn, *ibid.* 29 (1991).
[6] For a review, see M. L. Lee, E. A. Fitzgerald, M. T. Bulsara, M. T. Currie, and A. Lochtefeld, J. Appl. Phys. **97**, 011101 (2005).
[7] For a review, see B. Voigtländer, Surf. Sci. Rep. **43**, 127 (2001).
[8] D. J. Eaglesham and M. Cerullo, Phys. Rev. Lett. **64**, 1943 (1990).
[9] M. Hammar, F. K. LeGoues, J. Tersoff, M. C. Reuter, and R. M. Tromp, Surf. Sci. **349**, 129 (1996).
[10] J. Bernholc, N. O. Lipari, and S. T. Pantelides, Phys. Rev. Lett. **41**, 895 (1978); Phys. Rev. B **21**, 3545 (1980).
[11] G. A. Baraff and M. Schlüter, Phys. Rev. Lett. **41**, 892 (1978); Phys. Rev. B **19**, 4965 (1979).
[12] A. Fazzio, A. Janotti, A. J. R. da Silva, and R. Mota, Phys. Rev. B **61**, R2401 (2000).
[13] For a review, see G. D. Watkins, in *Deep Centers in Semiconductors*, edited by S. T. Pantelides (Gordon and Breach, New York, 1986), p. 147.
[14] O. Sugino and A. Oshiyama, Phys. Rev. Lett. **68**, 1858 (1992).
[15] G. D. Watkins and J. W. Corbett, Phys. Rev. **138**, A543 (1965); J. W. Corbett and G. D. Watkins, *ibid.* **138**, A555 (1965).
[16] M. Saito and A. Oshiyama, Phys. Rev. Lett. **73**, 866 (1994).
[17] S. Pöykkö, M. J. Puska, and R. M. Nieminen, Phys. Rev. B **53**, 3813 (1996).
[18] H. Seong and L. J. Lewis, Phys. Rev. B **53**, 9791 (1996).
[19] M. Pesola, J. von Boehm, S. Pöykkö, and R. M. Nieminen, Phys. Rev. B **58**, 1106 (1998).
[20] S. Öğüt and J. R. Chelikowsky, Phys. Rev. Lett. **83**, 3852 (1999).
[21] S. Öğüt and J. R. Chelikowsky, Phys. Rev. B **64**, 245206 (2001).
[22] D. V. Makhov and L. J. Lewis, Phys. Rev. B **72**, 073306 (2005).
[23] J.-I. Iwata, A. Oshiyama, and K. Shiraishi, Physica B **376-377**, 196 (2006).

[24] J. Coutinho, V. J. B. Torres, R. Jones, A. Carvalho, S. Öberg, and P. R. Briddon, Appl. Phys. Lett. **88**, 091919 (2006).
[25] P. Hohenberg and W. Kohn, Phys. Rev. **136**, B864 (1964).
[26] W. Kohn and L. J. Sham, Phys. Rev. **140**, A1133 (1965).
[27] D. M. Ceperley and B. J. Alder, Phys. Rev. Lett. **45**, 566 (1980).
[28] J. P. Perdew and A. Zunger, Phys. Rev. B **23**, 5048 (1981).
[29] J. P. Perdew, J. A. Chevary, S. H. Vosko, K. A. Jackson, M. R. Pederson, D. J. Singh, and C. Fiolhais, Phys. Rev. B **46**, 6671 (1992).
[30] N. Troullier and J. L. Martins, Phys. Rev. B **43**, 1993 (1991).
[31] G. P. Schwartz, M. S. Hybertsen, J. Bevk, R. G. Nuzzo, J. P. Mannaerts, and G. J. Gualtieri, Phys. Rev. B **39**, 1235 (1989).
[32] J. Almeida, L. Sirigu, G. Margaritondo, P. Da Padova, C. Quaresima, and P. Perfetti, J. Phys. D **32**, 191 (1999).
[33] C. G. Van de Walle and R. M. Martin, Phys. Rev. B **34**, 5621 (1986).
[34] D. V. Makhov and L. J. Lewis, Phys. Rev. Lett. **92**, 255504 (2004).
[35] The formation energy of V_1 in bulk Ge obtained by our 216-site supercell calculations (2.7 eV) is much larger than the value (1.9 eV) previously obtained in LDA approximation (Ref. 12). The reason for the discrepancy is unclear. Yet, when we rely on a dangling-bond counting model, the formation energy of an ideal V_1 becomes $E_{\mathrm{bond}}N_{\mathrm{DB}}/2=E_{\mathrm{coh}}$, with E_{bond}, N_{DB}, and E_{coh} being the bond energy, the number of dangling bonds generated by V_1, and the cohesive energy of the host material, respectively. When we take the value of the cohesive energy of 4 eV for Ge, the formation energy of V_1 is estimated to be 4 eV, which is close to our calculated value of 3.5 eV for the unrelaxed V_1.
[36] The energy gap of the Ge/Si slab in the present calculation is about 0.6 eV, with the calculated valence-band offset, the band gap in Si layers, and the band gap in Ge layers being 0.7, 1.3, and 0.8 eV, respectively. The calculated energy gaps of Si and Ge layers become larger than the corresponding values in bulk Si and Ge due to quantum confinement in a thin atomic slab.
[37] T. Matsushita, W. Sakai, K. Nakajima, M. Suzuki, K. Kimura, A. Agarwal, H.-J. Gossmann, and M. Ameen, Nucl. Instrum. Methods Phys. Res. B **230**, 230 (2005).
[38] T. Akiyama, Y. Okamoto, M. Saito, and A. Oshiyama, Jpn. J. Appl. Phys., Part 2 **38**, L1363 (1999).
[39] T. Akiyama and A. Oshiyama, J. Phys. Soc. Jpn. **70**, 1627 (2001).